GEOLOGY | THE GEOLOGICAL SOCIETY OF AMERICA®

https://doi.org/10.1130/G45608.1

Manuscript received 17 September 2018
Revised manuscript received 11 December 2018
Manuscript accepted 10 January 2019

High curvatures drive river meandering

Zoltán Sylvester[1], Paul Durkin[2], and Jacob A. Covault[1]
[1]Bureau of Economic Geology, Jackson School of Geosciences, The University of Texas at Austin, Austin, Texas 78758, USA
[2]Department of Geological Sciences, University of Manitoba, Winnipeg, Manitoba R3T 2N2, Canada

ABSTRACT

One of the long- and widely held ideas about the dynamics of meandering rivers is that migration slows down in bends with higher curvatures. High-resolution measurements of migration rates of more than 1600 bends in time-lapse Landsat satellite images, covering more than 4000 km of seven rapidly migrating meandering rivers in the Amazon Basin, suggest that the variation of migration rate closely follows that of the local channel curvature. However, locations of maximum migration rate are shifted downstream relative to peak curvature, with a phase lag that shows limited variability for the same river segment. A quasi-linear relationship exists between the two if this lag is taken into account. Overall, bends with the highest curvatures show the highest migration rates; exceptions with limited migration seem to be related to the low erodibility of the outer bank, not the hydrodynamics of the flow. The implication is that one of the most important ways river migration is rejuvenated and meandering patterns are reshuffled is the generation of high-curvature bends through cutoffs.

INTRODUCTION

Meandering rivers are among the most dynamic sedimentary systems on Earth. Meander bends of large rivers, especially ones with high sediment discharge, can migrate several meters per year (Constantine et al., 2014). Understanding and predicting how meanders change through time have major implications for a myriad of engineering and geological problems, including management of agricultural land, loss of infrastructure, bridge design, and distribution of heterogeneities in porous sediments and sedimentary rocks. The meandering process consists of erosion on the outer bank and deposition on the inner bank, which are the result of an asymmetric distribution of flow velocity and shear stress in curved channel segments (e.g., Dietrich et al., 1979). Inertial forces drive the high-velocity core of the river toward the outer bank; the strength of this effect is dependent on the bend curvature (e.g., Leopold and Wolman, 1960). In theory, the larger the curvature ($1/R$, where R is the radius of curvature), the larger is the centrifugal force and the shear stress exerted on the outer bank. Therefore, bends with high curvature should also have the highest migration rates. However, early studies of the relationship between curvature and migration rate suggested that migration rate reaches its highest value when the radius of curvature is about two to three times the width of the river (W; Hickin and Nanson, 1975; Nanson and Hickin, 1983, 1986). High-curvature bends with an R/W value < 2 appeared to migrate more slowly, potentially due to a higher energy expenditure and the development of a separation zone on the upstream side of the bend (Hickin, 1978). In parallel with these field measurements, theoretical work has clearly shown that the velocity excess at the outer bank depends not only on the local curvature, but it is also a function of the weighted sum of upstream curvatures (Ikeda et al., 1981; Howard and Knutson, 1984; Furbish, 1988). The integration of upstream curvatures results in a phase lag between curvature and migration rate, and this phase lag has not been considered in most previous studies. Although Furbish (1988) argued that migration rate is a monotonic function of curvature if bend length is taken into account, the idea that high-curvature bends show limited migration persists and is frequently explored in field studies, despite the increasing scatter in the plot of bend-averaged migration rate versus R/W as more data points are added (e.g., Knighton, 1998; Hudson and Kesel, 2000; Lagasse et al., 2004; Hooke, 2007; Sylvester and Covault, 2016; Finotello et al., 2018; Strick et al., 2018). High curvatures also seem to be associated with low migration rates in numerical modeling results (Crosato, 2009).

Although significant progress has recently been made in understanding the impact of sediment discharge on bend-averaged migration rates between different rivers (Constantine et al., 2014) and as a result of cutoffs (Schwenk and Foufoula-Georgiou, 2016), the bend-scale variability of migration rates has received limited attention. Time-lapse satellite imagery provides an opportunity to reevaluate the relationship between curvature and migration rate at a temporal and spatial resolution that was not possible before. Therefore, we digitized channel centerlines from Landsat satellite images of seven rivers in the Amazon Basin and estimated local migration rates through correlating centerlines.

DATA AND METHODS

Rivers of the Amazon Basin that drain the Andes have high water and sediment discharges and are among the fastest-migrating meandering rivers on Earth (Constantine et al., 2014). Tributaries with low-relief drainage basins are migrating at slower rates, but they still show a measurable change over the last ~30 yr, the time period for which Landsat imagery is available. Here, we focused on nine segments of seven rivers (Fig. 1) that show only limited contact with the edges of their incised valleys, which are usually locations with a significant reduction in erodibility compared to the alluvium deposited inside the valley (e.g., Nicoll and Hickin, 2010). For each river, we selected the time intervals between the two scenes as a function of overall migration rate. Channel banks and centerlines were digitized using a quasi-automated workflow based on the Rivamap river analysis and mapping Python package (Isikdogan et al., 2017). Migration rates were calculated using a dynamic time warping algorithm (e.g., Lisiecki and Lisiecki, 2002) that correlates each point along the first channel centerline to the closest point on the second centerline. These point-by-point measurements were taken at 25 m intervals.

To evaluate these measurements in a kinematic context, it is useful to summarize some key characteristics of the meandering process. A fundamental aspect of the meandering phenomenon is that the location of maximum migration does not coincide with the bend apex (e.g., Seminara, 2006); instead, it is often located

CITATION: Sylvester, Z., Durkin, P., and Covault, J.A., 2019, High curvatures drive river meandering: Geology, https://doi.org/10.1130/G45608.1

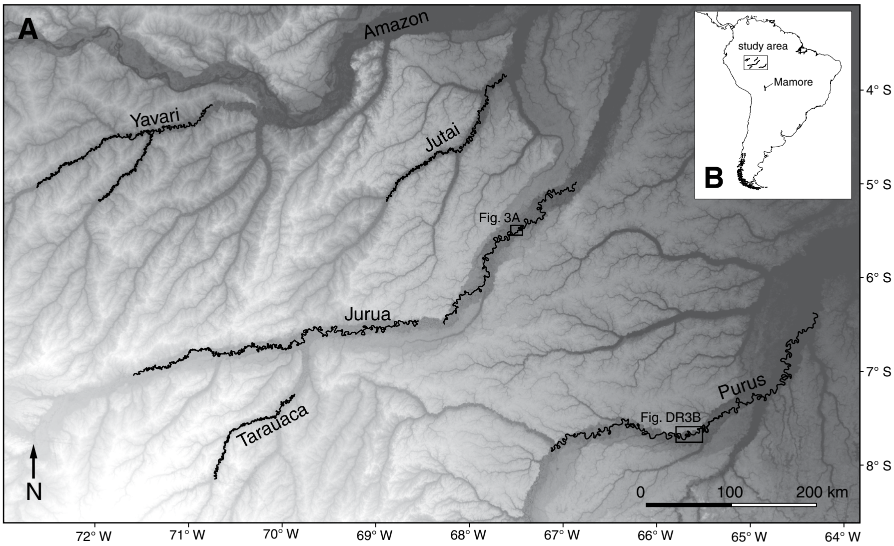

Figure 1. A: Locations of river segments used in our analysis. B: Location of study area in South America. Mamoré River segment is further south and is not shown on main map. Background map is based on Shuttle Radar Topography Mission (SRTM) elevation data; darker shades represent lower elevations.

downstream of the point of maximum curvature. This idea can be best illustrated using the concept of "nominal migration rate" (Fig. 2; Howard and Knutson, 1984), which is the migration rate that would be expected if bank erosion were only a function of local curvature. For the purpose of this study, we simplified the approach adopted by Howard and Knutson (1984) and defined the nominal migration rate as the product of the dimensionless curvature (W/R) and the migration rate constant k_1:

$$R_0 = k_1 W/R. \qquad (1)$$

Predicted migration rates can be estimated as the weighted sum of upstream curvatures:

$$R_1(s) = \Omega R_0(s) + \left[\Gamma\int_0^{\infty} R_0(s-\xi)G(\xi)d\xi\right]\left[\int_0^{\infty} G(\xi)d\xi\right]^{-1}, \qquad (2)$$

where Ω and Γ are weighting parameters with values of –1 and 2.5, s is the current location along the centerline, ξ is the along-channel distance upstream from that location, and $G(\xi)$ is an exponential weighting function:

$$G(\xi) = e^{-\alpha\xi}, \qquad (3)$$

where α is a function of friction factor C_f and water depth D, and k is a constant that equals 1:

$$\alpha = 2kC_f/D. \qquad (4)$$

Using this approach, and assuming a constant value for D for each river segment, we can optimize the value of C_f so that the phase shift between the actual and predicted migration curves is at a minimum. Then, the migration rate constant k_1 can be estimated by minimizing the difference between the absolute values of the actual and predicted migration rates. Migration rates that would be expected with the simplest meandering model can be estimated using Equation 2. Because large tributaries can significantly change both the water and sediment discharge, and these have an impact on migration rates (Constantine et al., 2014), we split all of the rivers into a few segments that did not include large tributaries.

When measuring migration rates in bends that have a strong translational component, it is important to consider the difference between bank migration and bend migration (Figs. 2B and 2C). "Bank migration" refers to the rate of bank erosion and accretion measured along a direction perpendicular to the banks or the centerline. Bend migration can be measured by linking points of similar curvature on the two centerlines, and it is significantly different from bank migration in bends showing downstream translation. In this study, we focused on bank migration, the primary physical process behind meandering, and a key component of the model used here.

Data and code (Jupyter notebooks) are available at https://github.com/zsylvester/curvaturepy. See the GSA Data Repository[1] for full results and more detail on the methods used.

---

[1] GSA Data Repository item 2019095, additional details of the methodology, and full results of the data analysis, is available online at http://www.geosociety.org/datarepository/2019/, or on request from editing@geosociety.org.

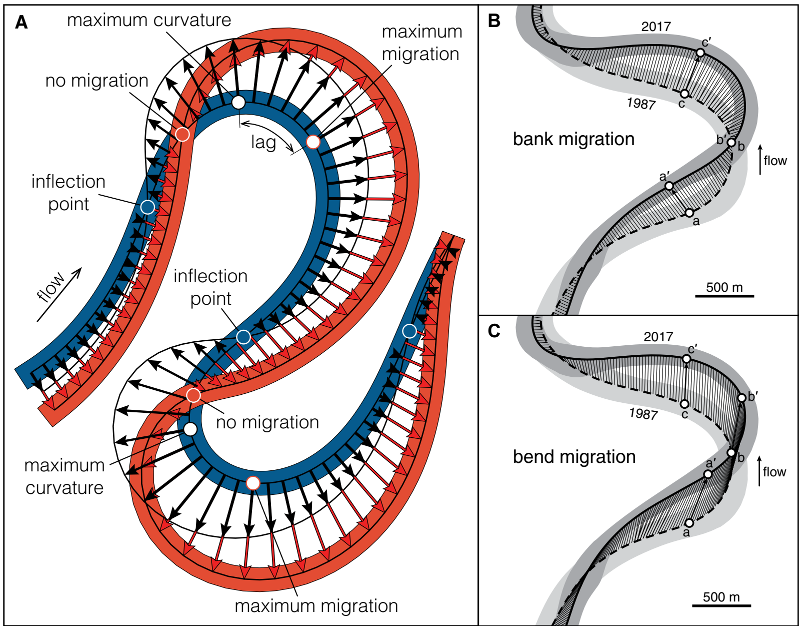

Figure 2. A: Nominal (black arrows) and predicted (red arrows) migration rates plotted along two meander bends, showing downstream delay of predicted migration rate relative to bend curvature. Phase lag corresponds to along-channel distance between locations of maximum curvature and maximum migration, which is roughly same as the distance between an inflection point and next point of no migration. B: Example of estimated bank migration vectors between two centerlines. Every point on centerline from A.D. 1987 is correlated to a point on centerline from 2017, minimizing distance between points, using dynamic time warping. Point of no migration is stationary (b is the same as b′). This is the approach in this study. C: Migration vectors that correspond to "bend migration," in a bend that shows significant translation. Inflection points correlate to inflection points. In this interpretation, the point where two centerlines cross each other ("point of no migration") moves ~500 m, from b to b′.

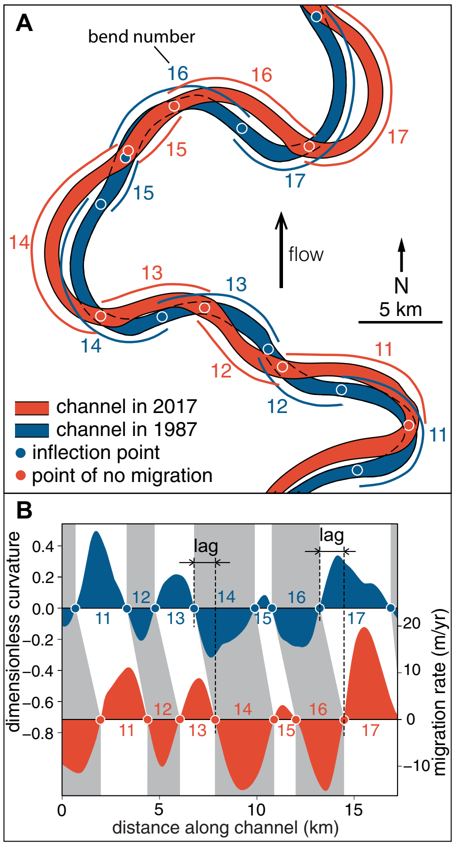

Figure 3. A: Channel locations of a short segment of Juruá River (Amazon Basin) in A.D. 1987 (blue) and in 2017 (red). Migration that is related to curvatures of bends defined on 1987 channel (blue arcs) is manifested downstream, in segments defined by points of no migration (red arcs). B: Curvature for 1987 channel (blue) and migration rate between 1987 and 2017 (red) along same segment of Juruá River. Bend numbers are same as in A. Note similarity between two curves and downstream shift of migration rate relative to curvature. See the Data Repository (see footnote 1) material for similar plots for all river segments.

RESULTS

The curvature and migration rate series are remarkably similar to each other for all river segments, although there are some obvious departures. We use a short segment of the Juruá River to illustrate the point-by-point relationship between the two series (Fig. 3). Although the nature of the change in channel locations is not immediately obvious in map view, a plot of the curvature and migration rate series side by side highlights their similarity and the need to consider the phase lag (Fig. 2) when trying to understand the relationship between the two. In the case of the Juruá River, the mean phase lag is 1073 m, with a standard deviation of 269 m. The phase lag shows a relatively low variability for the same river segment but varies between 2.1× and 4.7× the average channel width across different rivers. Virtually all bends show a downstream shift of the maximum migration rate relative to the bend apex.

If this phase lag is accounted for, both the nominal and predicted migration rates correlate well with the measured (actual) migration rates, for all river segments, with mean Pearson's *r* correlation coefficients of 0.76 and 0.75, respectively (Fig. 4; Table DR1). The scatter slightly increases at larger values, but there is no indication that migration rates would decrease beyond a critical high curvature.

Instead, there are significant numbers of data points that have anomalously large migration rates. A visual inspection of rapidly migrating high-curvature bends suggests that the majority are located downstream of recent cutoffs (green dots in Fig. 4). Most of the tight bends with potential separation zones along the upstream concave banks also fall into this category; that is, they do not show reduced migration rates. Low migration rates would be expected if the idea of increased flow resistance applied (Hickin and Nanson, 1975). The number of data points with lower than expected migration rates is also significant (red dots in Fig. 4). Part of this variability is likely due to the overall heterogeneous nature of the bank material (Güneralp and Rhoads, 2011). However, in many cases, the cause of the reduced migration rates can be more explicitly identified. Meanders that are impinging on erosional scarps related to river incision (red dots in right-side panels of Fig. 4) suggest that these low migration rates are caused by a reduction in erodibility associated with the edges of incised valleys. These edges and the related low-migration bends can be easily recognized in topographic maps derived from Shuttle Radar Topography Mission (SRTM) elevation data.

IMPLICATIONS FOR RIVER MEANDERING

Previous work has demonstrated the importance of upstream curvatures (Ikeda et al., 1981; Howard and Knutson, 1984; Furbish, 1988; Güneralp and Rhoads, 2009), variations in bank erodibility (Sun et al., 1996; Güneralp and Rhoads, 2011; Bogoni et al., 2017), and changes in sediment discharge (Constantine

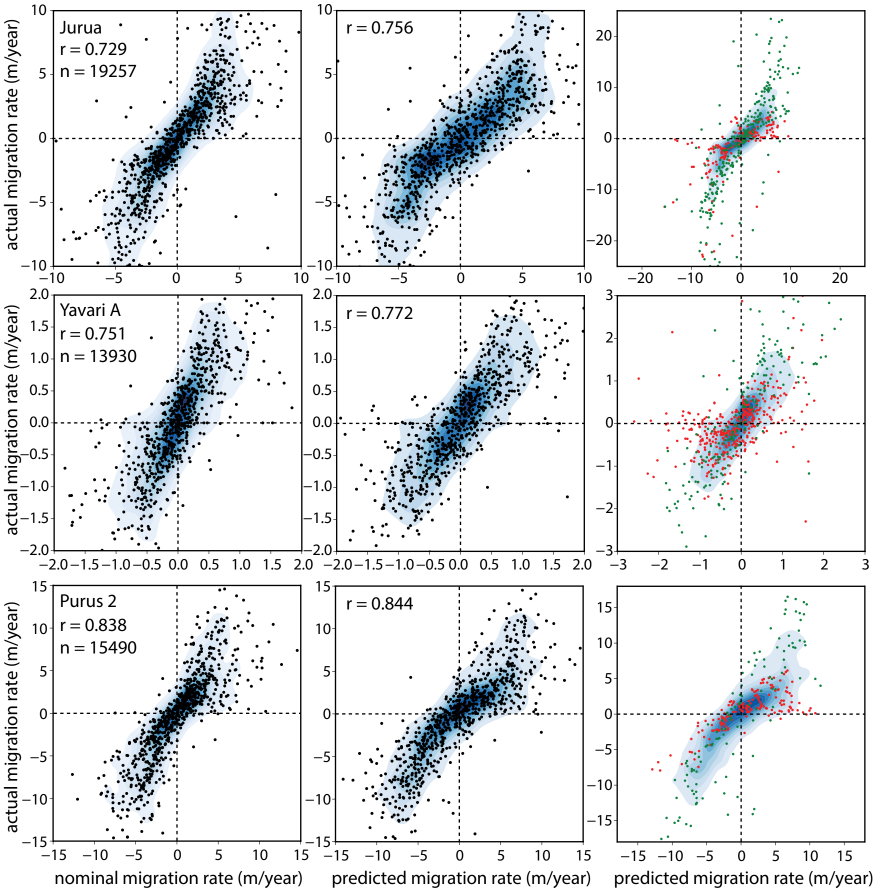

Figure 4. Plots of actual migration rate against nominal migration rate—corrected for phase lag—and predicted migration rates for three segments of Juruá, Yavarí, and Purus Rivers (Amazon Basin). Only 20% of data points are plotted as black dots. Areas shaded in blue are contour maps (with equal contour spacing) of bivariate kernel density estimate that includes all data points. In panels on right, green dots mark bends that seem to be affected by recent cutoffs; red dots are locations where migration is influenced by low-erodibility incised valley boundaries. See the Data Repository (see footnote 1) material for plots for all river segments.

et al., 2014; Schwenk and Foufoula-Georgiou, 2016) when estimating migration rates. The simple kinematic model of meandering used in our analysis focuses only on the impact of upstream curvatures and cannot reproduce processes like compound meander formation without cutoffs (Frascati and Lanzoni, 2009) or upstream migration under "superresonant" conditions (Seminara et al., 2001). However, it has a small number of parameters and provides a simple yet powerful framework for the analysis of the curvature–migration rate relationship. Our results suggest that the link between meander curvature and migration rate is relatively simple. One of the important implications of this link is that meander cutoffs play a key role in rejuvenating river migration. Most meanders start out after a cutoff event as small, sharp bends that rapidly migrate downstream and later undergo a slower expansion associated with lower curvatures (see also Schwenk et al., 2015).

To summarize our findings, high-resolution estimates of channel migration along seven large, relatively rapidly migrating rivers in the Amazon Basin suggest that (1) there is a quasi-linear relationship between local curvature and migration rate; (2) as expected from theory, the locations of the maximum curvature and migration are separated by a lag that is roughly constant for each river segment; and (3) the migration is shifted downstream relative to bend curvature by a distance that is 2.1 to 4.7 times larger than the channel width. On average, 57% of the variance in migration rates is predicted by curvature alone if the phase lag is considered. For a 250-km-long segment of the Jutaí River, this proportion is 74%. Contrary to the idea that channel migration slows down at high curvatures, we find that some of the sharpest bends are the ones that migrate with the highest speed. Some of the bends that are related to recent cutoffs show anomalously large migration rates, and these anomalies support the observations of Schwenk and Foufoula-Georgiou (2016). Lower-than-expected migration rates seem to be related to the reduced erodibility of the boundaries of the incising meander belts. The simple curvature–migration rate relationship observed in these rivers is likely to break down in systems with chute cutoffs, midchannel bars, and ones that are affected by significant erodibility variations. High-resolution mapping of additional rivers from different settings is needed to understand the general applicability of our approach and our findings. However, our results do suggest that some of the classic examples of meandering rivers on Earth display surprisingly simple and predictable migration patterns, in contrast with widely held ideas about the complexity of meander kinematics.

ACKNOWLEDGMENTS

We are thankful for support by sponsors of the Quantitative Clastics Laboratory (http://www.beg.utexas.edu/qcl) and for discussions with Eitan Shelef, Richard Sech, Brian Willis, Tao Sun, Nick Howes, and Matt Wolinsky. Constructive and insightful comments by Jon Schwenk, two anonymous reviewers, and editor Mark Quigley significantly improved the manuscript.

REFERENCES CITED

Bogoni, M., Putti, M., and Lanzoni, S., 2017, Modeling meander morphodynamics over self-formed heterogeneous floodplains: Water Resources Research, v. 53, p. 5137–5157, https://doi.org/10.1002/2017WR020726.

Constantine, J.A., Dunne, T., Ahmed, J., Legleiter, C., and Lazarus, E.D., 2014, Sediment supply as a driver of river meandering and floodplain evolution in the Amazon Basin: Nature Geoscience, v. 7, p. 899–903, https://doi.org/10.1038/ngeo2282.

Crosato, A., 2009, Physical explanations of variations in river meander migration rates from model comparison: Earth Surface Processes and Landforms, v. 34, p. 2078–2086, https://doi.org/10.1002/esp.1898.

Dietrich, W.E., Smith, J.D., and Dunne, T., 1979, Flow and sediment transport in a sand bedded meander: The Journal of Geology, v. 87, p. 305–315, https://doi.org/10.1086/628419.

Finotello, A., Lanzoni, S., Ghinassi, M., Marani, M., Rinaldo, A., and D'Alpaos, A., 2018, Field migration rates of tidal meanders recapitulate fluvial morphodynamics: Proceedings of the National Academy of Sciences of the United States of America, v. 115, p. 1463–1468, https://doi.org/10.1073/pnas.1711330115.

Frascati, A., and Lanzoni, S., 2009, Morphodynamic regime and long-term evolution of meandering rivers: Journal of Geophysical Research, v. 114, p. F02002, https://doi.org/10.1029/2008JF001101.

Furbish, D.J., 1988, River-bend curvature and migration: How are they related?: Geology, v. 16, p. 752–755, https://doi.org/10.1130/0091-7613(1988)016<0752:RBCAMH>2.3.CO;2.

Güneralp, I., and Rhoads, B.L., 2009, Empirical analysis of the planform curvature-migration relation of meandering rivers: Water Resources Research, v. 45, p. W09424, https://doi.org/10.1029/2008WR007533.

Güneralp, I., and Rhoads, B.L., 2011, Influence of floodplain erosional heterogeneity on planform complexity of meandering rivers: Geophysical Research Letters, v. 38, p. L14401, https://doi.org/10.1029/2011GL048134.

Hickin, E., 1978, Mean flow structure in meanders of the Squamish River, British Columbia: Canadian Journal of Earth Sciences, v. 15, p. 1833–1849, https://doi.org/10.1139/e78-191.

Hickin, E.J., and Nanson, G.C., 1975, The character of channel migration on the Beatton River, northeast British Columbia, Canada: Geological Society of America Bulletin, v. 86, p. 487–494, https://doi.org/10.1130/0016-7606(1975)86<487:TCOCMO>2.0.CO;2.

Hooke, J.M., 2007, Complexity, self-organisation and variation in behaviour in meandering rivers: Geomorphology, v. 91, p. 236–258, https://doi.org/10.1016/j.geomorph.2007.04.021.

Howard, A.D., and Knutson, T.R., 1984, Sufficient conditions for river meandering: A simulation approach: Water Resources Research, v. 20, p. 1659–1667, https://doi.org/10.1029/WR020i011p01659.

Hudson, P.F., and Kesel, R.H., 2000, Channel migration and meander-bend curvature in the Lower Mississippi River prior to major human modification: Geology, v. 28, p. 531–534, https://doi.org/10.1130/0091-7613(2000)28<531:CMAMCI>2.0.CO;2.

Ikeda, S., Parker, G., and Sawai, K., 1981, Bend theory of river meanders. Part 1. Linear development: Journal of Fluid Mechanics, v. 112, p. 363–377, https://doi.org/10.1017/S0022112081000451.

Isikdogan, F., Bovik, A., and Passalacqua, P., 2017, RivaMap: An automated river analysis and mapping engine: Remote Sensing of Environment, v. 202, p. 88–97, https://doi.org/10.1016/j.rse.2017.03.044.

Knighton, D., 1998, Fluvial Forms and Processes: A New Perspective: Abingdon, UK, Routledge, 400 p.

Lagasse, P.F., Zevenbergen, L., Spitz, W., and Thorne, C., 2004, A Methodology for Predicting Channel Migration: NCHRP Web-Only Document, Project No. 24–16: Fort Collins, Colorado, Ayres Associates, v. 67, 214 p., https://doi.org/10.17226/23352.

Leopold, L.B., and Wolman, M.G., 1960, River meanders: Geological Society of America Bulletin, v. 71, p. 769–794, https://doi.org/10.1130/0016-7606(1960)71[769:RM]2.0.CO;2.

Lisiecki, L.E., and Lisiecki, P.A., 2002, Application of dynamic programming to the correlation of paleoclimate records: Paleoceanography, v. 17, p. 1049, https://doi.org/10.1029/2001PA000733.

Nanson, G.C., and Hickin, E.J., 1983, Channel migration and incision on the Beatton River: Journal of Hydraulic Engineering, v. 109, p. 327–337, https://doi.org/10.1061/(ASCE)0733-9429(1983)109:3(327).

Nanson, G.C., and Hickin, E.J., 1986, A statistical analysis of bank erosion and channel migration in western Canada: Geological Society of America Bulletin, v. 97, p. 497–504, https://doi.org/10.1130/0016-7606(1986)97<497:ASAOBE>2.0.CO;2.

Nicoll, T.J., and Hickin, E.J., 2010, Planform geometry and channel migration of confined meandering rivers on the Canadian prairies: Geomorphology, v. 116, p. 37–47, https://doi.org/10.1016/j.geomorph.2009.10.005.

Schwenk, J., and Foufoula-Georgiou, E., 2016, Meander cutoffs nonlocally accelerate upstream and downstream migration and channel widening: Geophysical Research Letters, v. 43, p. 12,437–12,445, https://doi.org/10.1002/2016GL071670.

Schwenk, J., Lanzoni, S., and Foufoula-Georgiou, E., 2015, The life of a meander bend: Connecting shape and dynamics via analysis of a numerical model: Journal of Geophysical Research–Earth Surface, v. 120, p. 690–710, https://doi.org/10.1002/2014JF003252.

Seminara, G., 2006, Meanders: Journal of Fluid Mechanics, v. 554, p. 271–297, https://doi.org/10.1017/S0022112006008925.

Seminara, G., Zolezzi, G., Tubino, M., and Zardi, D., 2001, Downstream and upstream influence in river meandering, Part 2. Planimetric development: Journal of Fluid Mechanics, v. 438, p. 213–230, https://doi.org/10.1017/S0022112001004281.

Strick, R.J.P., Ashworth, P.J., Awcock, G., and Lewin, J., 2018, Morphology and spacing of river meander scrolls: Geomorphology, v. 310, p. 57–68, https://doi.org/10.1016/j.geomorph.2018.03.005.

Sun, T., Meakin, P., Jøssang, T., and Schwarz, K., 1996, A simulation model for meandering rivers: Water Resources Research, v. 32, p. 2937–2954, https://doi.org/10.1029/96WR00998.

Sylvester, Z., and Covault, J.A., 2016, Development of cutoff-related knickpoints during early evolution of submarine channels: Geology, v. 44, p. 835–838, https://doi.org/10.1130/G38397.1.

Printed in USA